*Am J Physiol Endocrinol Metab* 314: E53–E65, 2018.
First published October 24, 2017; doi:10.1152/ajpendo.00108.2017.

**RESEARCH ARTICLE**

# Inactivation of SPAK kinase reduces body weight gain in mice fed a high-fat diet by improving energy expenditure and insulin sensitivity

**Ivan Torre-Villalvazo,[1]* Luz Graciela Cervantes-Pérez,[2]* Lilia G. Noriega,[1] Jose V. Jiménez,[3] Norma Uribe,[4] María Chávez-Canales,[5] Claudia Tovar-Palacio,[3] Braulio A. Marfil-Garza,[3] Nimbe Torres,[1] Norma A. Bobadilla,[3,5] Armando R. Tovar,[1] and Gerardo Gamba[3,5,6]**

[1]*Department of Nutrition Physiology, Instituto Nacional de Ciencias Médicas y Nutrición Salvador Zubirán, Mexico City, Mexico;* [2]*Department of Pharmacology, Instituto Nacional de Cardiología Ignacio Chávez, México City, Mexico;* [3]*Department of Nephrology and Mineral Metabolism, Instituto Nacional de Ciencias Médicas y Nutrición Salvador Zubirán, Mexico City, Mexico;* [4]*Department of Pathology, Instituto Nacional de Ciencias Médicas y Nutrición Salvador Zubirán, México City, Mexico;* [5]*Molecular Physiology Unit, Instituto de Investigaciones Biomédicas, Universidad Nacional Autónoma de México, Mexico City, Mexico; and* [6]*Tecnologico de Monterrey, Escuela de Medicina y de Ciencias de la Salud, Monterrey, Mexico*

Submitted 27 March 2017; accepted in final form 18 October 2017

**Torre-Villalvazo I, Cervantes-Pérez LG, Noriega LG, Jiménez JV, Uribe N, Chávez-Canales M, Tovar-Palacio C, Marfil-Garza BA, Torres N, Bobadilla NA, Tovar AR, Gamba G.** Inactivation of SPAK kinase reduces body weight gain in mice fed a high-fat diet by improving energy expenditure and insulin sensitivity. *Am J Physiol Endocrinol Metab* 314: E53–E65, 2018. First published October 24, 2017; doi:10.1152/ajpendo.00108.2017.—The STE20/SPS1-related proline-alanine-rich protein kinase (SPAK) controls the activity of the electroneutral cation-chloride cotransporters (SLC12 family) and thus physiological processes such as modulation of cell volume, intracellular chloride concentration $[Cl^-]_i$, and transepithelial salt transport. Modulation of SPAK kinase activity may have an impact on hypertension and obesity, as *STK39*, the gene encoding SPAK, has been suggested as a hypertension and obesity susceptibility gene. In fact, the absence of SPAK activity in mice in which the activating threonine in the T loop was substituted by alanine (SPAK-KI mice) is associated with decreased blood pressure; however its consequences in metabolism have not been explored. Here, we fed wild-type and homozygous SPAK-KI mice a high-fat diet for 17 wk to evaluate weight gain, circulating substrates and hormones, energy expenditure, glucose tolerance, and insulin sensitivity. SPAK-KI mice exhibit resistance to HFD-induced obesity and hepatic steatosis associated with increased energy expenditure, higher thermogenic activity in brown adipose tissue, increased mitochondrial activity in skeletal muscle, and reduced white adipose tissue hypertrophy mediated by augmented whole body insulin sensitivity and glucose tolerance. Our data reveal a previously unrecognized role for the SPAK kinase in the regulation of energy balance, thermogenesis, and insulin sensitivity, suggesting that this kinase could be a new drug target for the treatment of obesity and the metabolic syndrome.

glucose tolerance; hepatic steatosis; kinase; metabolic syndrome; obesity; STE20/SPS1-related proline-alanine-rich protein kinase; uncoupling protein 1

## INTRODUCTION

Obesity is a worldwide health problem that contributes to the development of many metabolic chronic diseases. Among them, insulin resistance, hepatic steatosis, hyperlipidemia, and hypertension are the main causes of morbi-mortality leading in the development of type 2 diabetes and cardiovascular diseases (39). Several studies have demonstrated the gradual appearance of hypertension with the increase in the body mass index (49). In these subjects, there is an increase in body fat, leading to adipocyte hypertrophy, which is associated with a change in the secretion of free fatty acids (FFA) and adipokines, many of them involved in the regulation of insulin sensitivity, lipid metabolism, and blood pressure regulation (48).

In a study using an integrated approach of comparative genomics between humans and pigs, in which 8,842 individuals from South Korea between 40 and 69 yr were studied, Kim et al. (23) reported that *STK39* affected hypertension and obesity traits, suggesting that *STK39* could be both a hypertension and obesity susceptibility gene (50). The *STK39* gene is located in chromosome 2 and codifies for the STE20/SPS1-related proline-alanine-rich protein kinase (SPAK) (15). In addition, in a previous study, the *SKT39* gene was also suggested as a susceptibility gene for the development of hypertension (52).

SPAK is a member of the germinal center kinase superfamily of serine/threonine kinases that is a major target of the upstream "with-no-lysine kinases" (WNK1-WNK4) (47) and, therefore, directly responsible for the phosphorylation of WNK targets, among which the most well known are the members of the electroneutral cation chloride-coupled cotransporters from the SLC12 family of solute carriers (17, 20).

The SLC12 family of cotransporters is divided into two branches: the $Na^+$ coupled to chloride branch that includes, $Na^+$-$Cl^-$ cotransporter (NCC) and two isoforms of the $Na^+$-$K^+$-$2Cl^-$ cotransporter, NKCC1 and NKCC2, and the $K^+$-coupled to chloride branch that comprises four isoforms of the $K^+$-$Cl^-$ cotransporters, KCC1 to KCC4 (5, 17). The coordinated activity of the SLC12 members culminates in a movement of ions inside or outside the cell in an electroneutral

* I. Torre-Villalvazo and L. G. Cervantes-Pérez contributed equally to this work.

Address for reprint requests and other correspondence: G. Gamba, Vasco de Quiroga No. 15, Tlalpan, 14080, Mexico City, Mexico (e-mail: gamba@biomedicas.unam.mx).

fashion and thus is important for a diversity of physiological processes, including modulation of cell volume, intracellular chloride concentration $[Cl^-]_i$, and transepithelial salt transport.

WNKs activate SPAK by promoting its phosphorylation in the threonine 243 at the T loop in mice, resulting in phosphorylation of the SLC12 cotransporters. SPAK knockin (SPAK-KI) mice carry a substitution of threonine 243 per alanine, and thus, SPAK kinase is expressed but not functional (37). Consistent with the role of SPAK in blood pressure modulation, SPAK-KI mice feature a salt loosing nephropathy phenotype with arterial hypotension that corrects with salt administration (37).

Recent evidence has shown that SPAK is expressed beside the kidney in white adipose tissue. Interestingly, a global phosphoproteomic analysis of white adipose tissue from mice fed a low-fat or a high-fat diet (HFD) identified differential phosphorylation levels in 282 phosphosites from 191 proteins, including SPAK (6). Given that our laboratory has studied the SPAK-KI mice, due to our interest in hypertension (9), the aim of the present work was to further characterize the role of SPAK in obesity by exposing these mice to a HFD and evaluating body composition, adiposity, hepatic lipid content, energy expenditure, glucose tolerance, and insulin sensitivity.

## MATERIALS AND METHODS

*Animals.* SPAK-KI mice were generated and maintained on an inbred C57BL/6J background, as previously described (37). To generate diet-induced obesity in mice, 10-wk-old male SPAK-KI mice and their wild-type C57BL/6J littermates were housed individually under controlled temperature (23 ± 2°C) with a 12:12-h light-dark cycle and constant humidity and fed a purified-ingredient high-fat diet (HFD; 45% kcal fat) or a purified-ingredient control diet (12% kcal fat), as previously described (26). All mice were given free access to diet and water for 17 wk according to standard procedures (36). Body weight was measured weekly. Individual average food intake was calculated by measuring food intake every other day along the study (in g). We then obtained the average consumption of daily food intake throughout the 17 wk of the study. Energy intake was estimated by multiplying food intake (g) per energy density of the control or HFD (3.87 or 4.68 kcal/g, respectively). At the end of the study, mice were food deprived for 6 h and euthanized by overdose of isofluorane. White and brown adipose tissues, liver, pancreas, soleus, and gastrocnemius skeletal muscles were rapidly excised, frozen in liquid nitrogen, and stored at −70°C. Blood was obtained from the posterior vena cava using a 1-ml syringe. Serum was separated by centrifugation for 10 min at 1,800 *g* at 4°C.

To evaluate insulin sensitivity, wild-type and SPAK-KI mice fed a control diet were food deprived for 6 h and received 1 IU/kg of insulin (Humulin R; Eli Lilly) or saline intraperitoneally. After 20 min, liver, skeletal muscle, and retroperitoneal adipose tissue were collected and stored as previously mentioned above. All animal procedures were conducted in accordance with National Institutes of Health Guidelines (NIH) for the Care and Use of Animals and approved by the Animal Ethics Research Committee of the Instituto Nacional de Ciencias Médicas y Nutrición Salvador Zubirán.

*Body composition and indirect calorimetry measurement.* Body composition (lean and fat mass) was evaluated at *week 14* on their corresponding diet using magnetic resonance (EchoMRI; Echo Medical Systems, Houston, TX). According to the manufacturers of the EchoMRI system, the lean mass is a muscle tissue mass equivalent to all of the body parts containing water, excluding fat, bone minerals, and such substances that do not contribute to the NMR signal, such as hair, claws, etc. Therefore, most of the total water is already included in lean mass and so counted twice in the sum of fat, lean, and total water. Energy expenditure analysis was assessed by indirect calorimetry using the Oxymax CLAMS system (Comprehensive Laboratory Animal Monitoring System, Columbus, OH). After 15 wk on their corresponding diet, mice were acclimatized for 24 h before data collection. Mice were food deprived for 6 h for fasting recordings and then feeding with their corresponding diets for the next 18 h. Oxygen consumption and $CO_2$ production were continuously measured throughout the test. Respiratory exchange ratio (RER) was calculated as the volume of $CO_2$ exhaled ($\dot{V}_{CO_2}$; $ml \cdot kg^{-1} \cdot h^{-1}$) divided by the volume of $O_2$ inhaled ($\dot{V}_{O_2}$; $ml \cdot kg^{-1} \cdot h^{-1}$).

*Glucose metabolism studies.* Intraperitoneal glucose tolerance test (IPGTT) and insulin tolerance test (ITT) were performed in 22-wk-old mice after 12 or 13 wk on their corresponding diet, as previously described (38). Blood glucose levels were measured with a portable blood glucose meter (ACCU-CHEK; Roche Diagnostics, Indianapolis, IN). The homeostasis model assessment index of insulin resistance (HOMA-IR) was determined using the following formula: [insulin (mU/l) × glucose (mmol/l)/22.5] (29). To determine plasma insulin concentration, blood samples were obtained at *time 0*, *15*, and *30 min* during IPGTT in wild-type and SPAK-KI mice fed a control diet.

*Biochemical and hormonal variables.* Plasma cholesterol and triglyceride concentrations were determined using an automated clinical chemistry analyzer (cobas c 111; Roche). Plasma insulin and leptin were measured by ELISA (EMD Millipore, Darmstadt, Germany). Plasma free fatty acids (FFA) concentration was assayed with a Roche FFA kit (Roche), and plasma free glycerol was determined with a colorimetric assay (Sigma, St. Louis, MO).

*Histological, immunofluorescent, and immunohistochemical analyses.* Paraffin-embedded, dewaxed 4-μm sections of brown adipose tissue (BAT), white adipose tissue (WAT), and liver were stained with hematoxylin and eosin (H & E) using standard protocols. For uncoupling protein 1 (UCP1) immunofluorescence analysis, paraffin-embedded BAT samples were cut at 4 μm, deparaffinized, and rehydrated. Slides were incubated for 20 min at 90°C in sodium citrate buffer for epitope retrieval, and sections were permeabilized with 0.1% Triton X-100 in PBS blocked with 10% rabbit serum, followed by incubation with the primary antibody against UCP1 (ab23841; Abcam, Cambridge, MA). Sections were washed for 3 × 5 min in PBS and incubated with Alexa Fluor 488 goat anti-rabbit IgG (Molecular Probes by Life Technologies). All incubations were performed at room temperature for 60 min. The sections were rinsed for 3 × 5 min in PBS and coverslips mounted with Prolong Gold antifade reagent with DAPI (Molecular Probes). The staining was visualized with a Leica fluorescent microscopy system. Relative quantification was performed using ImageJ Software, as described (4). Data were expressed as fluorescence intensity in arbitrary units. Immunohistochemistry of chromogranin A (CgA) in pancreas was determined by incubation with biotinylated primary CgA (ab15160; Abcam) antibody according to the avidin-biotin complex method (21). Negative control staining was performed with normal donkey serum diluted 1:100 instead of primary antibody. To visualize neutral lipids, frozen liver and skeletal muscle sections (8 μm) were stained with Oil Red O (ORO; Sigma) and counterstained with hematoxylin. To evaluate mitochondrial activity in skeletal muscle, we performed a succinate dehydrogenase (SDH) histochemical assay, as previously described (26). The densitometric quantitation of SDH, ORO staining, and morphometric analysis of islet areas was performed using the ImageJ software (NIH), as described previously (26, 31, 44). The number and size of adipocytes in histological sections were quantified using the Adiposoft software, as described (16).

*RNA extraction and mRNA quantitation.* Total RNA from BAT was extracted with TRIzol reagent (Invitrogen; Thermo Fisher Scientific, Waltham, MA) and retrotranscribed using oligo(dT) 12–18 and M-MLV reverse transcriptase (Invitrogen). UCP1 and peroxisome proliferator-activated receptor (PPAR)-γ coactivator-1 (PGC-1) mRNA abundance was quantified using SybrGreen master mix in a LightCycler 480 Instrument (Roche). Samples were run in

triplicate, and data were analyzed by the second derivate maximum method. Target gene expression levels were normalized to hypoxanthine phosphoribosyltransferase mRNA abundance, as internal invariant control.

*INS1E cell culture.* INS1E cells were cultured in RPMI 1640 medium supplemented with 10% fetal calf serum, 1 mM sodium pyruvate, 50 μM 2-mercaptoethanol, 2 mM glutamine, 10 mM HEPES, 100 U/ml penicillin, and 100 μg/ml streptomycin. INS1E cells were seeded on 24-well plates and after 48 h incubated with hypotonic low-chloride buffer (HLC; 67.5 mM sodium gluconate, 2.5 mM potassium gluconate, 0.25 mM $CaCl_2$, 0.25 mM $MgCl_2$, 0.5 mM $Na_2HPO_4$, 0.5 mM $Na_2SO_4$, and 7.5 mM HEPES, pH 7.5) for 1 h to stimulate SPAK activity (32). To assess the effect of glucose on SPAK phosphorylation, INS1E cells were incubated with Krebs-Ringer bicarbonate buffer (135 mM NaCl, 3.6 mM KCl, 2 mM NaHCO3, 0.5 mM NaH2PO4, 0.5 mM MgSO4, 1.5 mM CaCl2, 10 mM HEPES, pH 7.4, and 0.1% bovine serum albumin) containing 2.5 or 25 mM glucose for 1 h. After incubation, cells were used for protein extraction, as indicated below.

*Protein extraction, SDS/PAGE, and immunoblotting.* Frozen BAT, liver, skeletal muscle, and cells were homogenized in ice-cold RIPA buffer with protease inhibitor cocktail (Complete; Roche) and phosphatase inhibitor cocktail (PhosSTOP; Roche), as described (38). Protein concentration was determined using the DC protein assay kit (Bio-Rad Laboratories, Richmond, CA). Tissue lysates (20 μg) were combined with Laemmli sample buffer and separated by SDS-PAGE. After electrophoretic separation, the proteins were electrotransferred to a PVDF membrane using a Trans-Blot SD Semi-Dry Electrophoretic Transfer Cell, and membranes were blocked in TBS-Tween 20 (TBST) containing 5% nonfat dry milk for 1 h and incubated overnight at 4°C with primary antibodies against UCP1 in BAT, Akt (sc-8312; Santa Cruz Biotechnology), and phosphorylated Akt ($Ser^{473}$, 9018; Cell Signaling Technology) in liver and skeletal muscle. The sheep antibodies anti-SPAK (total) and anti-SPAK phosphorylated $Thr^{243}$ (Division of Signal Transduction Therapy of the University of Dundee) were used at a concentration of 1 μg/ml in TBST containing 5% nonfat dry milk. The anti-sheep peroxidase-conjugated antibody (Santa Cruz Biotechnology) was also diluted in TBST with 5% nonfat dry, and membranes were incubated for 1.5 h at room temperature. Band detection was carried out using a chemiluminescent Western blotting kit (Immobilon Western Chemiluminescent HRP Substrate; Millipore). Digital images of the membranes were obtained by a ChemiDoc MP densitometer and processed using Image Laboratory software (Bio-Rad, Hercules, CA). Results are reported relative to β-actin. A value of 1 was arbitrarily assigned to the control samples, which were used as a reference for the other conditions.

*Statistical analysis.* The results are presented as means ± SE. Parameters measured over time (weight gain, oxygen consumption, RER, and glucose during IPGTT and ITT) were analyzed using repeated-measures analysis of variance (ANOVA; genotype × diet × time), followed by Bonferroni correction. Genotype and diet interactions (SPAK-KI vs. wild-type and control vs. HFD, respectively) were analyzed using a two-way ANOVA, followed by a Bonferroni multiple comparison post hoc test. Immunoblot densitometry data analysis involving three groups (wild-type + saline, wild-type + insulin and SPAK-KI + insulin) was analyzed by one-way ANOVA, followed by a Bonferroni multiple comparison post hoc test. Immunoblot densitometry data analysis involving two groups (control vs. HFD or wild-type vs. SPAK-KI) were performed using an unpaired Student's *t*-test. Statistical analysis was performed using GraphPad 6.0 (GraphPad, San Diego, CA). The letters used in the graphs indicate statistically significant difference ($P < 0.05$) between marked groups, where a > b > c.

## RESULTS

*Weight gain in response to HFD is prevented in SPAK-KI mice.* Wild-type and SPAK-KI mice were fed either a control diet or a HFD for 17 wk. At the beginning of the study, the length and weight of the wild-type and SPAK-KI mice were similar [length: 10.04 ± 0.16 vs. 9.90 ± 0.19 cm, $P$ = not significant (NS); weight: 29.73 ± 0.91 vs. 28.91 ± 1.05 g, $P$ = NS]. As expected, mice fed a control diet gained 3–4 g during the period of study regardless of the genotype (Fig. 1*A*). Wild-type mice fed a HFD significantly increased body weight with respect to mice fed a control diet. However, SPAK-KI mice fed a HFD exhibited significantly lower body weight gain than their wild-type littermates. At the end of the study period, body weight in SPAK-KI fed a HFD was on average 5 g lower than wild-type mice on the same diet ($P < 0.01$; Fig. 1*B*). To determine whether the difference in body weight between wild-type and SPAK-KI mice was due to differences in food intake, we measured food consumption throughout the study. Food intake (in g) was lower in both groups fed the HFD (Fig. 1*C*). However, because the HFD is more calorie dense than the control diet, food intake expressed as kilocalories per day was not different between groups (Fig. 1*D*). Fat mass was significantly higher in both groups of mice on HFD than those fed the control diet; however, SPAK-KI mice fed a HFD exhibited lower fat mass than wild-type mice (Fig. 1*E*). As shown in Fig. 1, *F* and *G*, lean mass and body water content were significantly lower in mice fed a HFD compared with those fed the control diet, and no difference was found between genotypes with either diet. Thus, the SPAK-KI mice fed the HFD accumulated less fat mass than their wild-type littermates, without significant change in food intake, leading to a lower body weight gain.

*SPAK-KI mice fed a HFD had lower circulating lipids and reduced hepatic lipid accumulation.* Plasma glucose was higher in both groups fed a HFD, with no difference between genotypes (Fig. 2*A*). Cholesterol and triglycerides were also higher in mice fed a HFD with respect to those fed the control diet; however, these parameters were significantly lower in SPAK-KI than in wild-type mice fed a HFD (Fig. 2, *B* and *C*). Serum leptin was higher in mice fed a HFD than those fed a control diet, but again, SPAK-KI showed a significant reduction in circulating leptin with respect to wild-type on the same diet (Fig. 2*D*). One of the earliest alterations observed during weight gain in response to a HFD is the development of hepatic steatosis (51). Thus, we evaluated liver morphology and hepatic lipid content. The liver histology of SPAK-KI mice fed a control diet was identical to that of wild-type mice (Fig. 2*E*). Wild-type mice on a HFD had macrovesicular steatosis in >80% of their hepatocytes, whereas SPAK-KI mice showed a morphology that was similar to both groups of mice on a control diet. Quantification of ORO staining confirms that SPAK-KI mice had lower hepatic steatosis than wild-type mice fed a HFD (Fig. 2*F*). Interestingly, we observed for the first time that SPAK is expressed in liver, and its content, surprisingly, is increased when animals are fed a HFD (Fig. 2*G*). These results suggest a potential role of this kinase in hepatic lipid metabolism, since the absence of SPAK activity prevented hepatic steatosis during a HFD, whereas in the wild-type mice there was an accumulation of hepatic lipids.

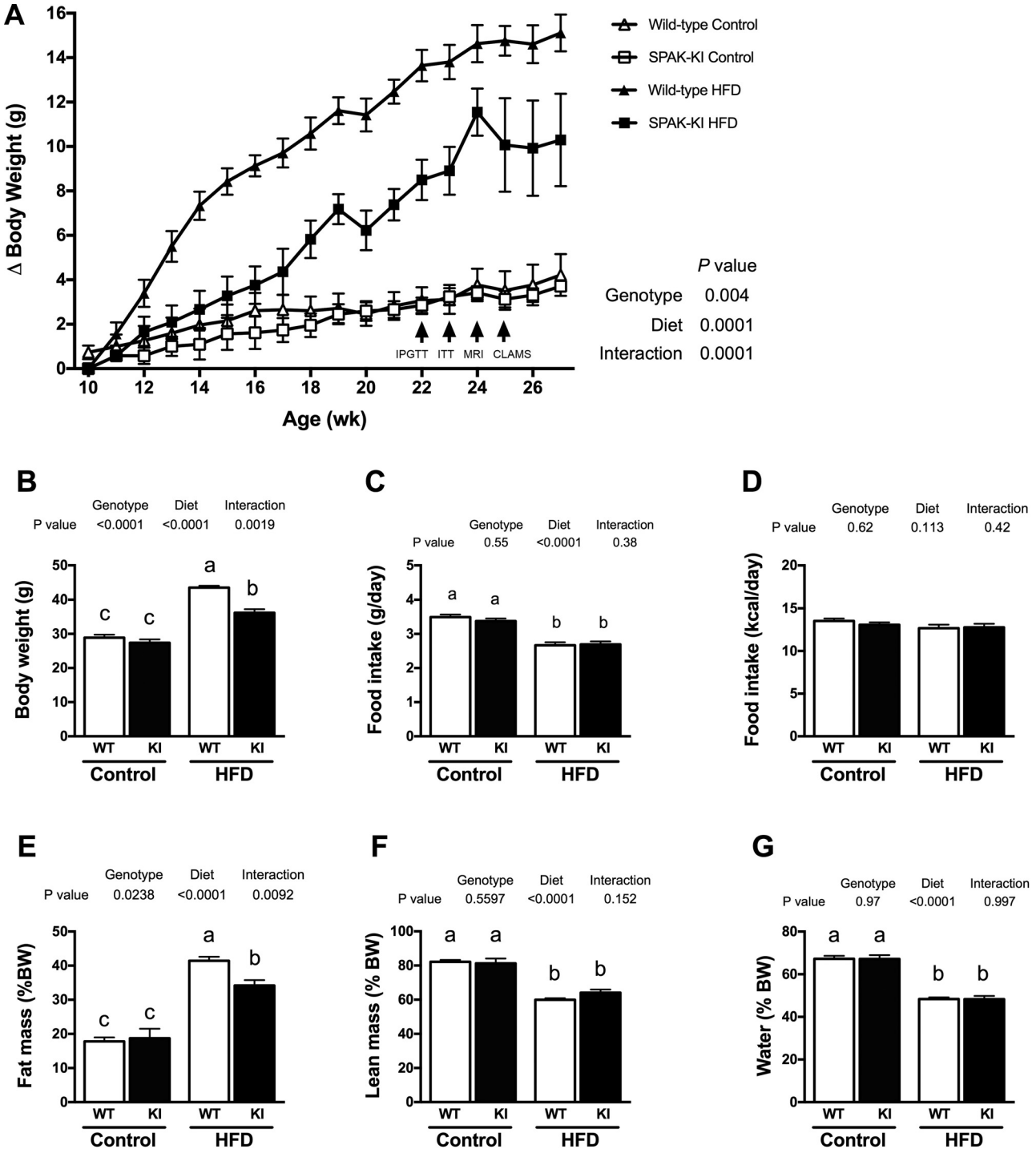


Fig. 1. High-fat diet-induced obesity is attenuated in STE20/SPS1-related proline-alanine-rich protein kinase knockin (SPAK-KI) mice. *A*: Δbody weight of mice fed for 17 wk a control diet (12% kcal/fat) or a high-fat diet (HFD; 45% kcal/fat). Arrows indicate when mice were subjected to intraperitoneal glucose tolerance test (IPGTT), insulin tolerance test (ITT), magnetic resonance (MRI), and indirect calorimetry using a Comprehensive Laboratory Animal Monitoring System (CLAMS). *B*: body weight at the end of the study. *C* and *D*: mean food intake in g/day (*C*) and in kcal/day (*D*) throughout the study period. *E–G*: body composition analysis: fat mass (*E*), lean mass (*F*), and total water (*G*) in SPAK-KI mice (black bars) and their wild-type littermates (open bars) after 14 wk of being fed a control diet or a HFD (as stated). %BW, %body weight. The results are presented as means ± SE. Weight gain over time was analyzed using 2-way ANOVA for repeated measures followed by Bonferroni correction. Genotype and diet interactions were analyzed using a 2-way parametric analysis of variance (ANOVA), followed by a Bonferroni multiple comparison post hoc test. Different letters denote significant difference between groups ($P < 0.05$), where a > b > c; $n = 8–10$ mice for each group.

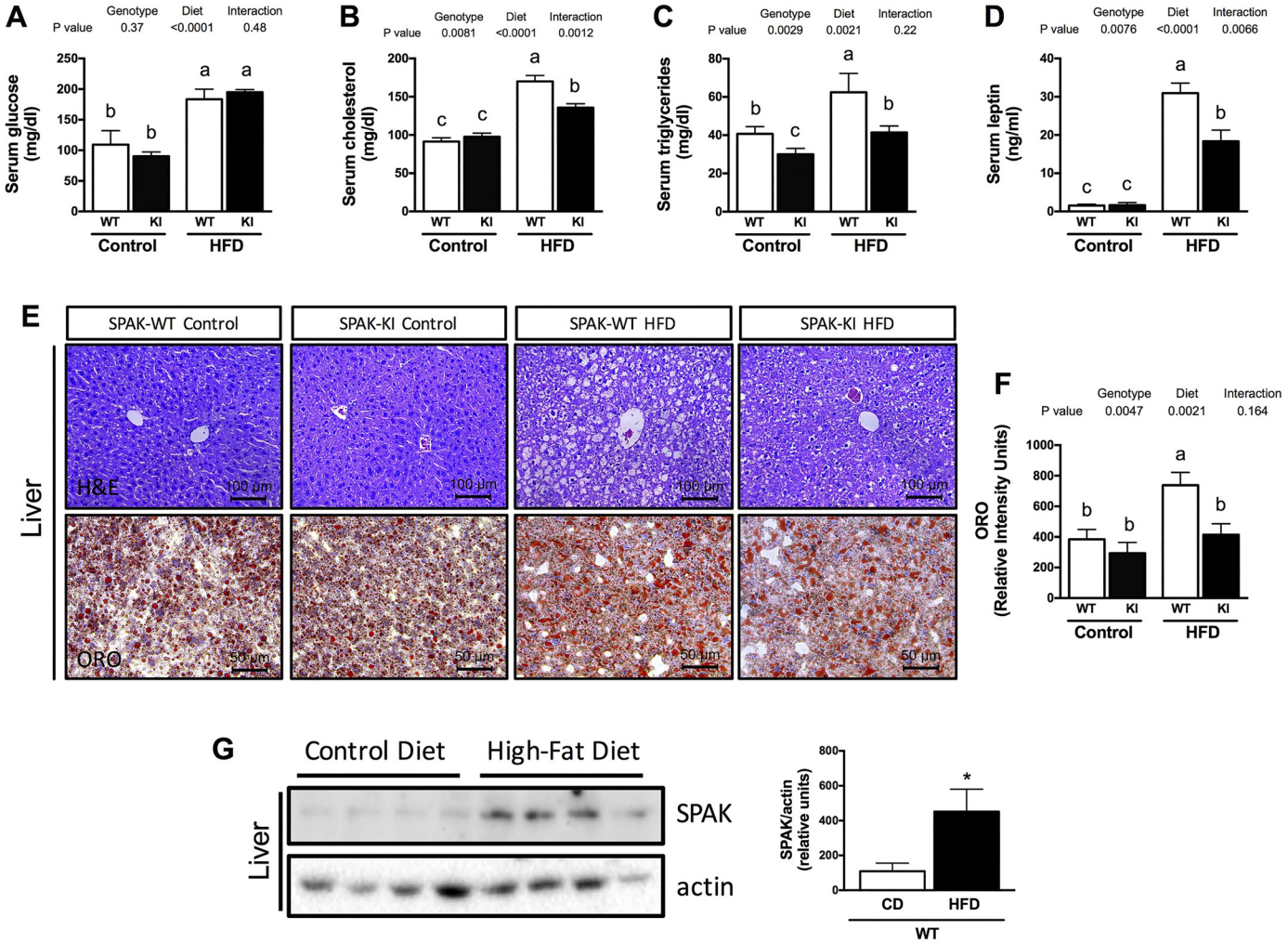


Fig. 2. SPAK-KI mice have lower serum lipids and reduced hepatic steatosis when fed a HFD. *A–F*: serum concentration of glucose (*A*), total cholesterol (*B*), triglycerides (*C*), leptin (*D*) and liver (*E*) sections stained with hematoxylin and eosin (H & E) and Oil Red O (ORO), and ORO hepatic staining quantitation (*F*) in SPAK-KI mice (black bars) and their wild-type littermates (open bars) after 17 wk of being fed a control diet or a HFD. *G*: SPAK protein content in liver of wild-type mice fed a control diet or HFD. Representative blots are shown. The bar graphs represent the mean ± SE of quantitative densitometry from 3 independent experiments. The results are presented as means ± SE. Genotype and diet interactions were analyzed using a 2-way parametric analysis of variance (ANOVA), followed by a Bonferroni multiple comparison post hoc test. Immunoblot densitometry data analysis was performed using an unpaired Student's *t*-test. Different letters denote significant difference between groups ($P < 0.05$), where a > b > c; $n = 8–10$ mice for each group.

*SPAK-KI mice on a HFD increased energy expenditure and UCP1 content in BAT.* To evaluate whether the lower body fat and hepatic lipid content in SPAK-KI mice on a HFD was associated with increased energy expenditure, we determined $O_2$ consumption by indirect calorimetry during *week 15* of dietary treatment. Average $O_2$ consumption was lower in wild-type mice fed a HFD diet compared with wild-type and SPAK-KI mice fed a control diet during the feeding period (night) (Fig. 3*A*). In SPAK-KI mice fed a HFD, average $O_2$ consumption during the feeding period was significantly higher compared with their wild-type littermates (Fig. 3*B*). To discard that the difference in $O_2$ consumption was due to total body weight differences, we also calculated $\dot{V}O_2$ consumption per kilogram of lean mass. After adjusting for this, $O_2$ consumption per kilogram of lean mass was still significantly higher in SPAK-KI mice with respect to wild-type mice fed a HFD (Fig. 3*C*). Our data showed that wild-type and SPAK-KI mice on a control diet had a similar respiratory exchange ratio (RER) of 0.98 during the feeding period, indicating that both groups relied almost exclusively on glucose oxidation (Fig. 3, *D* and *E*). In contrast, mice fed the HFD had greater fatty acid oxidation than mice fed the control diet; however, SPAK-KI mice were oxidizing more fat. In fact, according to the table of Lusk (28), SPAK-KI mice were oxidizing 68.3% of lipids, whereas wild-type mice were oxidizing 51.2% of lipids, as indicated by the RER of 0.84 and 0.80, respectively ($P < 0.05$) (Fig. 3*E*). Heat production during the feeding period was significantly higher in SPAK-KI mice fed a HFD compared with their wild-type littermates, indicating greater energy expenditure (Fig. 3*F*).

To determine whether the augmented energy expenditure and heat production in SPAK-KI mice fed a HFD was associated with brown adipose tissue (BAT) thermogenesis, we evaluated BAT morphology and UCP1 expression. Brown adipose tissue from wild-type and SPAK-KI mice on a control diet was composed of UCP1-positive multilocular adipocytes

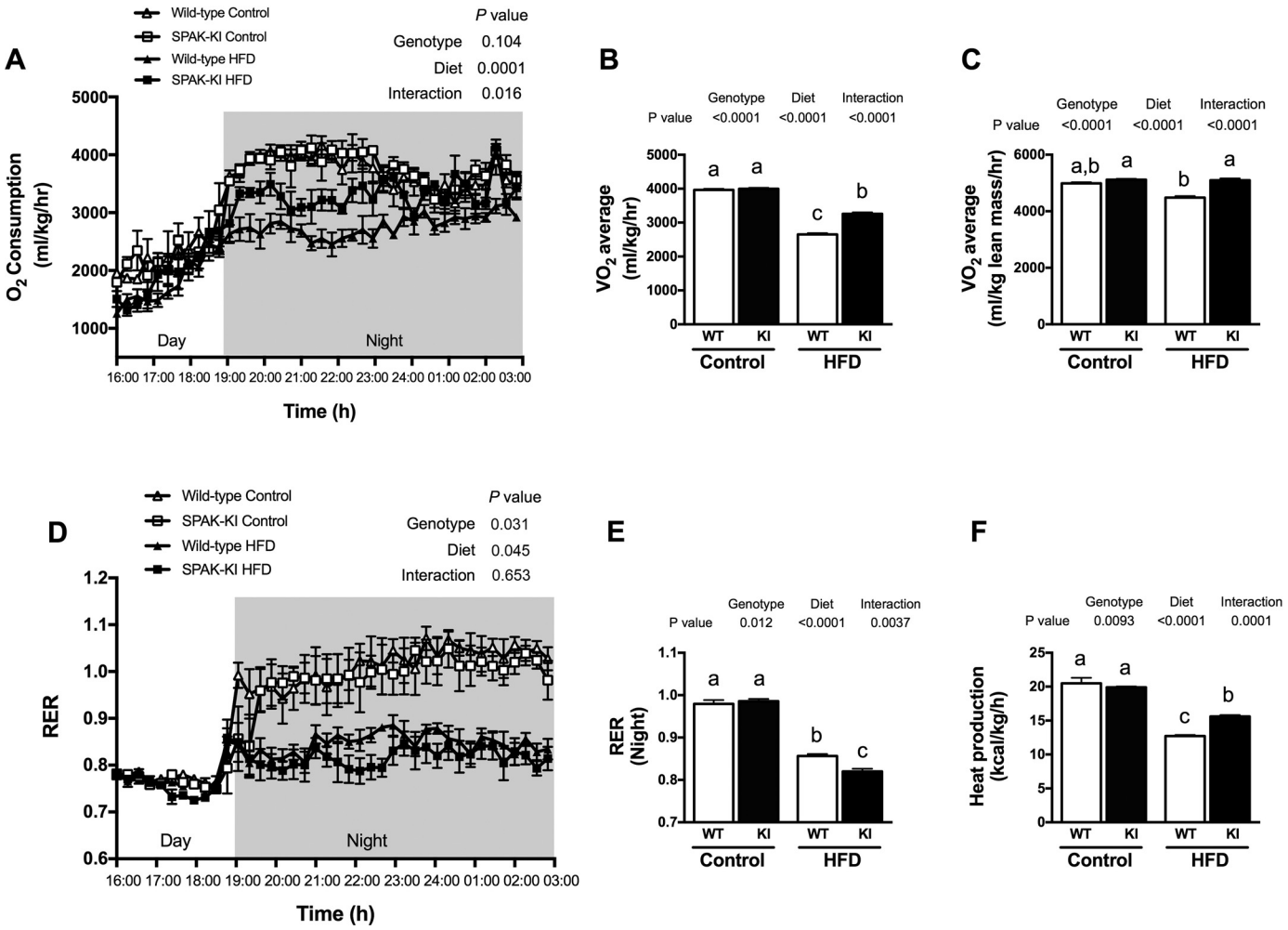


Fig. 3. SPAK-KI mice exhibit higher energy expenditure than wild-type mice when fed a HFD. $O_2$ consumption over a 13-h period (*A*), $\dot{V}O_2$ average normalized to total body weight (*B*), $\dot{V}O_2$ average normalized to lean mass (*C*), respiratory exchange ratio (RER) over a 13-h period (*D*), respiratory exchange ratio (RER) average during the night period (*E*), and heat production of SPAK-KI mice (black bars) and their wild-type littermates (open bars) after 15 wk of being fed a control diet or HFD (*F*). The results are presented as means ± SE. Oxygen consumption and RER over time were analyzed using 2-way ANOVA for repeated measures, followed by Bonferroni correction. Genotype and diet interactions were analyzed using a 2-way parametric analysis of variance (ANOVA), followed by a Bonferroni multiple comparison post hoc test. Different letters denote significant difference between groups ($P < 0.05$), where a > b > c; $n = 8$–10 mice for each group.

(Fig. 4, *A* and *B*). In contrast, wild-type mice on a HFD developed hypertrophic brown adipocytes with enlarged lipid droplets, a process observed during obesity referred to as "whitening" (18). Interestingly, BAT morphology of SPAK-KI mice fed a HFD resembles that observed in mice fed the control diet, indicating better lipid utilization (Fig. 4*A*). Furthermore, as shown in Fig. 4, *A*, *B*, and *E*, the UCP1 protein content measured by both immunefluorescence and Western blot was significantly augmented in BAT of SPAK-KI mice on a HFD compared with the rest of the groups. In addition, the UCP1 mRNA content was also higher in SPAK-KI mice compared with wild-type mice, along with increased PPARγ coactivator-1α (PGC1α) mRNA content (Fig. 4, *C* and *D*). Western blot analysis also revealed that SPAK-KI mice fed a HFD had a significant higher amount compared with the wild-type mice. However, this difference was less evident in mice of both genotypes fed the control diet. The difference between UCP1 mRNA and protein content observed in wild-type mice fed a HFD can be due to increased protein stability, as was previously demonstrated by Chouchani et al. (10). These findings strongly suggest that the lower weight gain in the SPAK-KI mice compared with wild-type mice in response to a HFD was in part due to increased thermogenesis in BAT.

*Inactivation of SPAK increased mitochondrial activity in skeletal muscle and prevented white adipocyte hypertrophy in mice fed a HFD.* Alterations in energy balance during obesity are associated with decreased mitochondrial oxidative capacity in skeletal muscle, leading to impaired substrate oxidation and intramyocellular lipid accumulation (33). Thus, we determined the succinate dehydrogenase (SDH) activity and lipid content (ORO) in the gastrocnemius muscle. As expected, wild-type mice fed a HFD had lower SDH activity and increased ORO staining in muscle fibers compared with those fed a control diet (Fig. 5, *A*–*C*). Surprisingly, SDH activity and ORO staining in SPAK-KI mice fed a HFD were similar to those of groups fed a control diet. These results indicate that SPAK-KI mice challenged with a HFD increased oxygen consumption in part

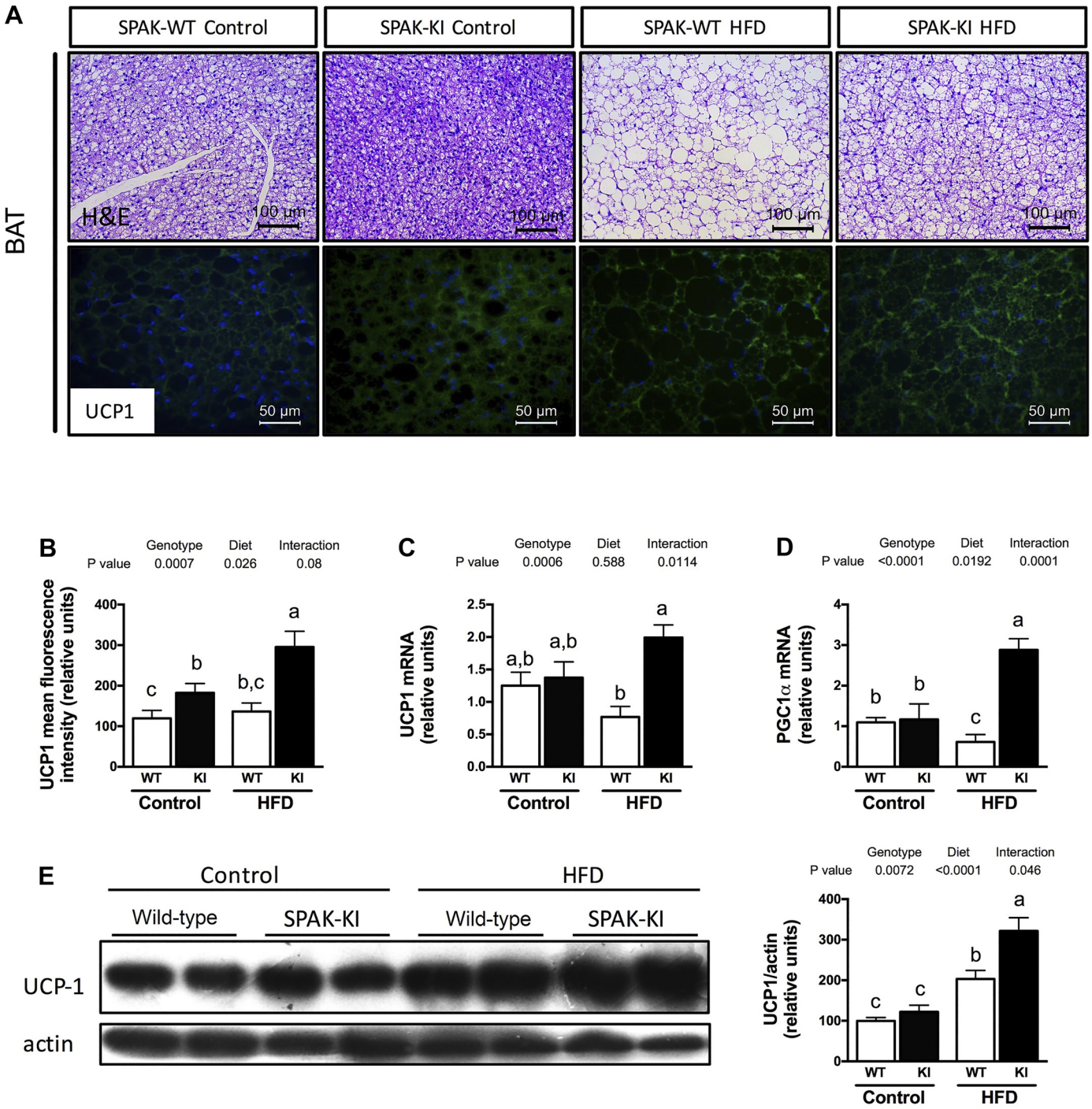


Fig. 4. Uncoupling protein 1 (UCP1) content is increased in BAT of SPAK-KI mice fed a HFD. *A*: brown adipose tissue (BAT) H & E staining and UCP1 immunofluorescence. *B–D*: mean fluorescence intensity (*B*), UCP1 mRNA (*C*), and PPARγ coactivator-1α (PGC-1α) mRNA content (*D*). *E*: UCP1 protein content in BAT of SPAK-KI mice (black bars) and their wild-type littermates (open bars) after 17 wk of being fed a control diet or a HFD. Representative blots are shown. The bar graphs represent means ± SE of quantitative densitometry from 3 independent experiments. The results are presented as means ± SE. Genotype and diet interactions were analyzed using a 2-way parametric analysis of variance (ANOVA), followed by a Bonferroni multiple comparison post hoc test. Different letters denote significant difference between groups ($P < 0.05$), where a > b > c; $n = 8–10$ mice for each group.

by enhancing mitochondrial activity and fatty acid oxidation in skeletal muscle.

The main source of circulating free fatty acids (FFA) during obesity is dysregulated lipolysis in WAT, which occurs in parallel with adipocyte hypertrophy (12, 34). White adipocytes from wild-type and SPAK-KI mice fed a control diet were similar in size (Fig. 5, *A* and *D*). As expected, adipocytes from wild-type mice on a HFD were significantly larger than those in the control group, indicating adipocyte hypertrophy. As shown in Fig. 5*D*, the average adipocyte size of SPAK-KI mice fed a HFD was smaller than that of wild-type mice on the same diet. In accord with the histological findings, plasma FFA were

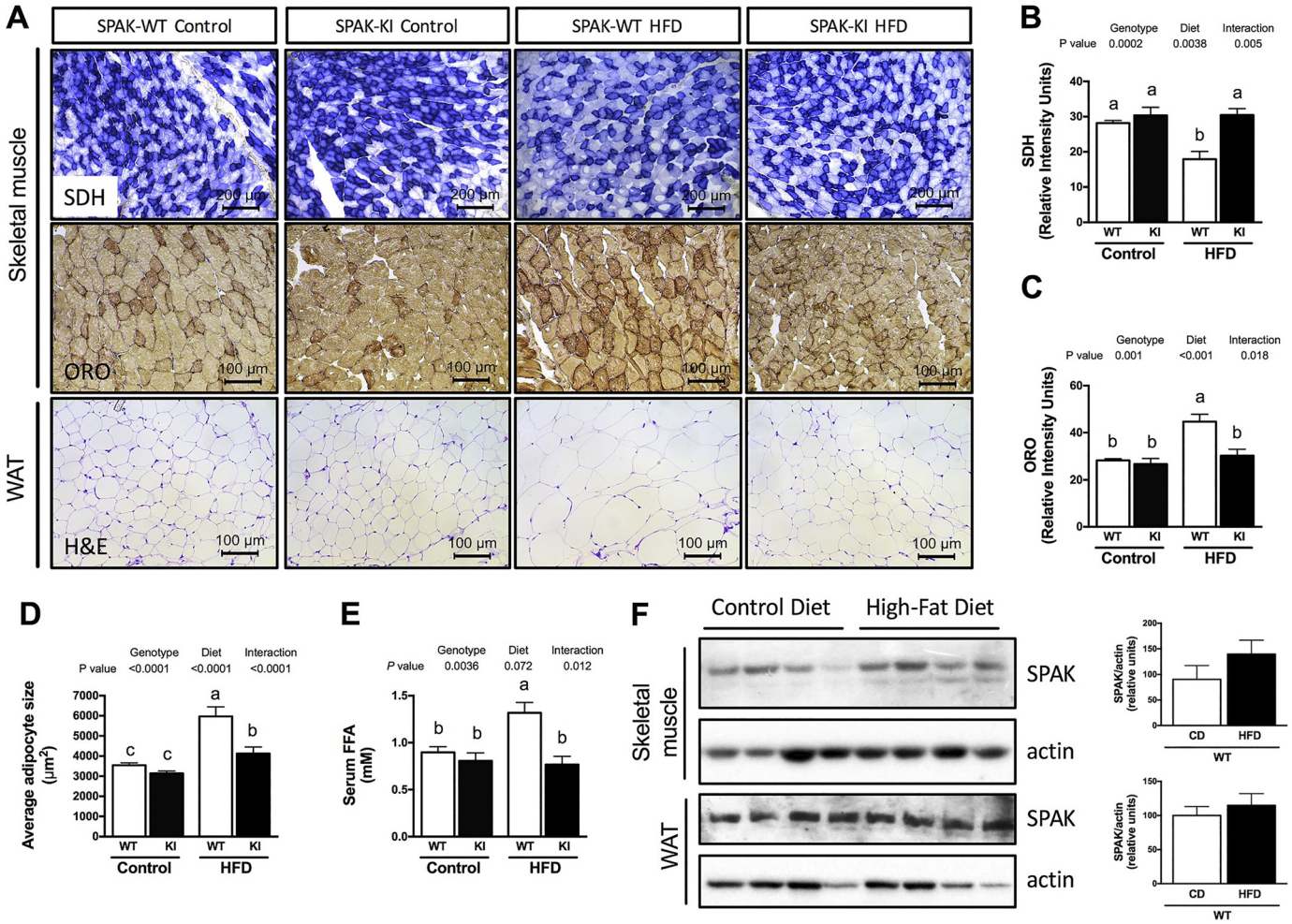


Fig. 5. SPAK kinase inactivation increases skeletal muscle mitochondrial activity and prevents white adipose tissue (WAT) hypertrophy in mice fed a HFD. *A*: succinate dehydrogenase (SDH) activity and Oil red O (ORO) staining in skeletal muscle and H & E staining of white adipose tissue (WAT). *B* and *C*: SDH (*B*) and ORO staining (*C*) quantitative densitometry. *D* and *E*: WAT average adipocyte area (*D*) and plasma free fatty acids (*E*) of SPAK-KI mice (black bars) and their wild-type littermates (open bars) after 17 wk of being fed a control diet or HFD. *F*: SPAK protein content in skeletal muscle and WAT of wild-type mice fed a control diet or HFD. Representative blots are shown. The bar graphs represent the mean ± SE of quantitative densitometry from 3 independent experiments. The results are presented as means ± SE. Genotype and diet interactions were analyzed using a 2-way parametric analysis of variance (ANOVA), followed by a Bonferroni multiple comparison post hoc test. Immunoblot densitometry data analysis was performed using an unpaired Student's *t*-test. Different letters denote significant difference between groups ($P < 0.05$), where a > b > c; $n = 8$–10 mice for each group.

higher in wild-type mice fed a HFD compared with those fed a control diet (Fig. 5*E*). Interestingly, circulating FFA in SPAK-KI mice on a HFD were similar to that of both groups fed the control diet. These results indicate that the absence of SPAK activity prevents adipocyte hypertrophy on a HFD. Consistent with a potential role of SPAK in skeletal muscle and in WAT, we observed that these tissues exhibit SPAK expression, although no changes were observed during HFD (Fig. 5*F*).

*SPAK inactivity prevented pancreatic islet hypertrophy in mice fed a HFD.* Chronic elevated fat intake is directly associated with insulin resistance and hyperinsulinemia (30, 45). The increased insulin requirement during insulin resistance to maintain euglycemia causes islet hypertrophy (35). Accordingly, wild-type mice fed a HFD exhibited marked hypertrophy of the pancreatic islets associated with hyperinsulinemia and elevated HOMA-IR index (Fig. 6, *A*–*D*). Interestingly, SPAK-KI mice fed a HFD presented a significant reduction in islet area along with reduced plasma insulin concentration and HOMA-IR compared with wild-type mice. It is worth noticing that even in a control diet, the mean islet area of SPAK-KI mice is significantly lower than that observed in wild-type mice (Fig. 6*B*).

*SPAK inactivity improved glucose tolerance associated with lower insulin levels during IPGTT.* To assess the effect of a HFD on glucose metabolism in SPAK-KI mice, we performed an intraperitoneal glucose tolerance test (IPGTT) at *week 12* of dietary treatment (Fig. 7*A*) During the IPGTT, mice fed a HFD showed a reduction in glucose tolerance, as indicated by an increased area under the curve (Fig. 7*B*). Interestingly, SPAK-KI mice showed an improved glucose tolerance in both control and HFD when compared with their wild-type littermates, as indicated by a lower area under the curve than their wild-type littermates (Fig. 7, *A* and *B*). The improved glucose tolerance could be associated with an improvement in insulin sensitivity in SPAK-KI mice. In fact, the plasma insulin concentration during the IPGTT was lower in SPAK-KI mice fed a control diet than in wild-type mice

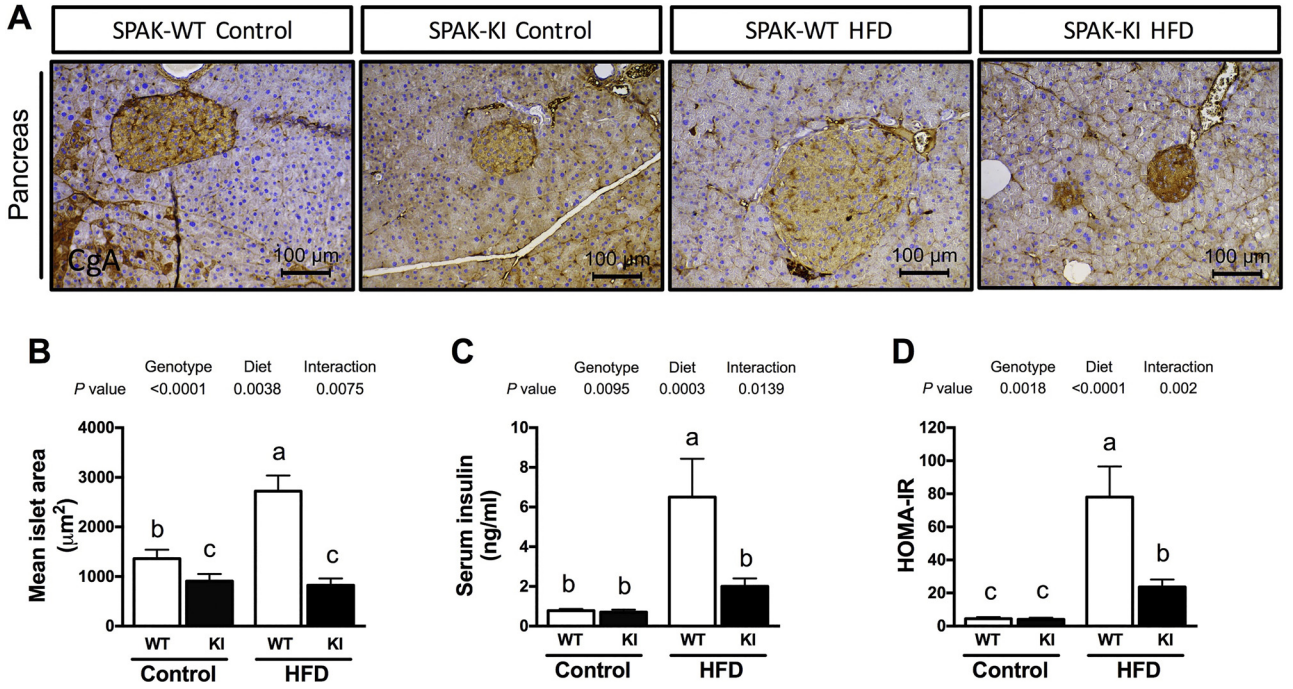


Fig. 6. Pancreatic islet area and homeostasis model index of insulin resistance (HOMA-IR) are reduced in SPAK-KI mice fed a HFD. Chromogranin A (CgA) immunohistochemistry in pancreas sections (*A*), morphometric analysis of islet areas (*B*), serum insulin concentration (*C*), and HOMA-IR of SPAK-KI mice (black bars) and their wild-type (WT) littermates (open bars) (*D*) after 17 wk of being fed a control diet or HFD. The results are presented as means ± SE. Genotype and diet interactions were analyzed using a 2-way parametric analysis of variance (ANOVA), followed by a Bonferroni multiple comparison post hoc test. Different letters denote significant difference between groups ($P < 0.05$), where a > b > c; $n = 8$–10 mice for each group.

(Fig. 7*C*), suggesting an improvement of insulin sensitivity by SPAK inactivation.

We also evaluated the expression and phosphorylation of SPAK kinase on pancreatic β-cells. To this end, the insulin-secreting cell line INS1E was incubated in control and in hypotonic low-chloride buffer (HLC), a known stimulator of SPAK activity, or in high-glucose Krebs-Ringer (HG) buffer. We observed that the INSE1 cells express SPAK, and its phosphorylation in $Thr^{243}$ increased with the hypotonic low-chloride buffer and the HG buffers (Fig. 7*D*). These results suggest that SPAK may modulate plasmatic insulin levels, on the one hand, through a possible effect on insulin secretion by β-cells and, on the other hand, by an improvement of whole body insulin sensitivity.

Therefore, we performed an insulin tolerance test (ITT) to evaluate whole body insulin sensitivity in wild-type and SPAK-KI mice. As depicted in Fig. 8*A*, wild-type mice fed a HFD presented a significantly blunted response to a single intraperitoneal injection of 0.5 U/kg insulin, with no decrease in blood glucose throughout the test. Interestingly, circulating glucose in SPAK-KI mice fed a HFD exhibited a significant reduction after 30 min of insulin administration, as observed in mice fed a control diet, which returned to basal concentrations 120 min postinjection. This result suggests that SPAK-KI mice have improved insulin sensitivity. Furthermore, we obtained liver and gastrocnemius muscle from mice in control diet after a 20-min injection of insulin to evaluate the phosphorylation of Akt. Interestingly, SPAK KI mice had higher levels of phosphorylated Akt in both liver and muscle, confirming improved intracellular insulin signaling (Fig. 8*B*).

## DISCUSSION

This study provides evidence that SPAK inactivation reduces weight gain and adiposity in mice fed a HFD compared with wild-type mice despite similar food intake. The reduction in adipose tissue mass was associated with improved skeletal muscle mitochondrial content and increased UCP1-mediated thermogenesis in BAT, leading to increased whole body oxygen consumption and heat production. In addition, the SPAK-KI mice had better insulin sensitivity and reduced pancreatic islet area, which helped to reduce the effect of HFD on hyperglycemia and hepatic lipid production.

Diet-induced obesity produces profound derangements in energy metabolism (19). As expected, wild-type mice fed a HFD developed fatty liver and BAT hypertrophy and lower energy expenditure associated with higher circulating levels of cholesterol, TG, glucose intolerance, higher basal insulin levels, insulin resistance, and hypertrophy of pancreatic islets. Notably, all of these parameters were attenuated in the SPAK-KI mice. The fact that the increase in many of the metabolic parameters associated with obesity was significantly lower in SPAK-KI mice than their wild-type littermates under the same diet along the weeks is likely due to lower adiposity. Indeed, because circulating leptin levels are directly associated with the adipose tissue mass (14), the decrease in serum leptin observed in SPAK-KI mice is a clear indicator of the lower increase in body fat according to the assessment of magnetic resonance compared with wild-type mice fed a high-fat diet, explaining the reduced body weight gain in SPAK-KI mice.

Our data support that the improved energy metabolism of SPAK-KI mice involves at least two different mechanisms

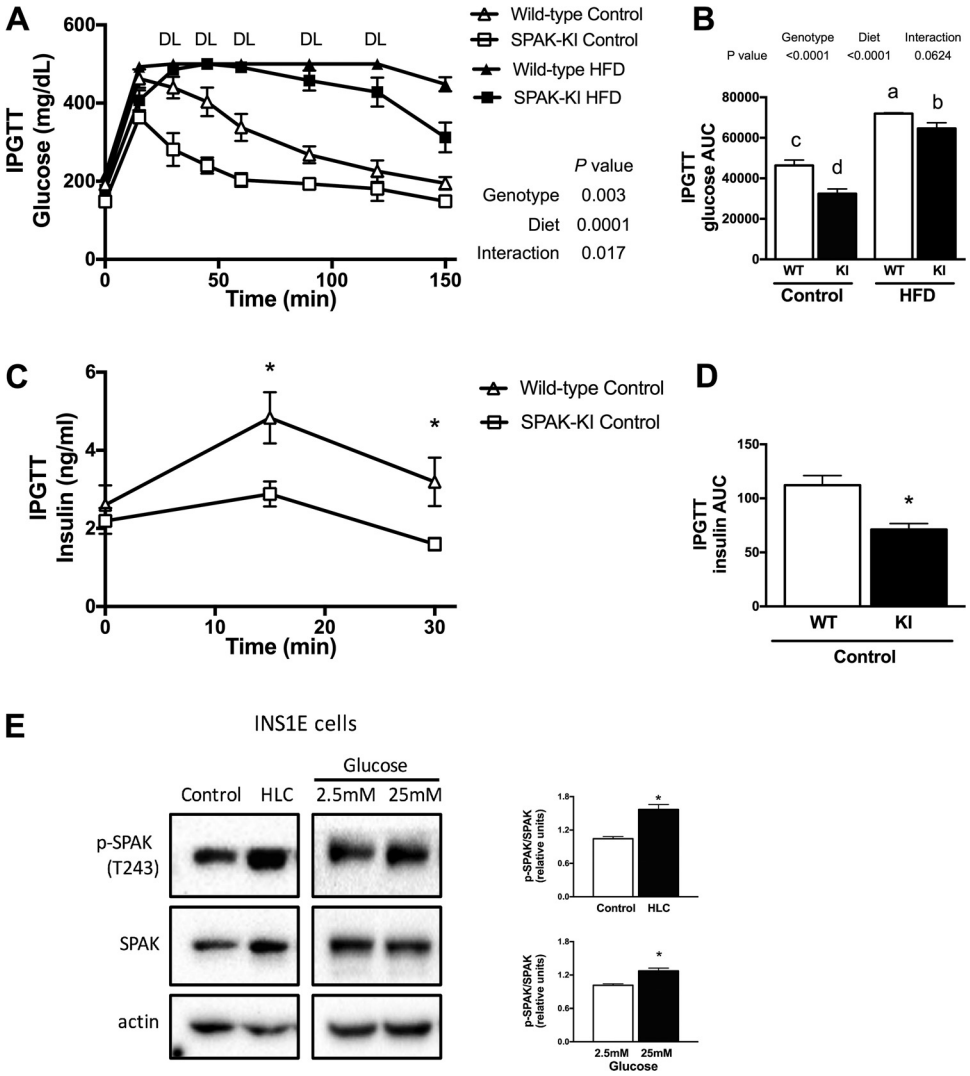


Fig. 7. SPAK-KI mice exhibit increased glucose tolerance associated with lower insulin levels during an IPGTT. SPAK phosphorylation increases in insulin-secreting INS1E cells in response to a hypotonic low-chloride or a high-glucose buffer. *A* and *B*: glucose concentration during the IPGTT (*A*) and glucose area under the curve (AUC) during the IPGTT in SPAK-KI mice (black bars) and their wild-type littermates (open bars) after 12 wk of being fed a control diet or HFD (*B*). *C* and *D*: insulin concentration during the IPGTT (*C*) and insulin AUC of wild-type and SPAK-KI mice fed a control diet (*D*). *E*: SPAK phosphorylation in $Thr^{243}$ in INS1E cells incubated in control or hypotonic low-chloride (HLC) buffer and a low (2.5 mM) or high (25 mM) glucose buffer. Representative blots are shown. The bar graphs represent mean ± SE of quantitative densitometry from 3 independent experiments. The results are presented as means ± SE. Glucose and insulin concentrations over time data during the IPGTT were analyzed using 2-way ANOVA for repeated measures, followed by Bonferroni correction. Genotype and diet interactions were analyzed using a 2-way parametric analysis of variance (ANOVA), followed by a Bonferroni multiple-comparison post hoc test. Insulin AUC and immunoblot densitometry data analysis was performed using an unpaired Student's *t*-test. Different letters denote significant difference between groups ($P < 0.05$), where a > b > c; $n$ = 8–10 mice for each group.

(Fig. 9). One is only apparent when mice are fed a HFD and the other is present even when mice are fed a control diet. In the first mechanism, during HFD the SPAK-KI mice exhibited higher energy expenditure evaluated by higher $O_2$ consumption that was associated with increased UCP1 expression in BAT and higher mitochondrial content in skeletal muscle. These parameters are not different between wild-type and SPAK-KI mice fed control diet. Thus, SPAK-KI mice maintain increased energy expenditure when fed a HFD, and as consequence, the SPAK-KI mice have reduced adiposity that leads to a lessening of obesity by ~15% during chronic HFD. Interestingly, the increase in energy expenditure caused by the lack of SPAK activity is only apparent when mice are challenged with a HFD. This situation resembles human conditions in which, beyond genetic susceptibility, exposure to the appropriate environment is required for the phenotype to become evident (22).

The second mechanism, however, is apparent even when mice are fed a control diet. During the IPGTT, we observed that SPAK-KI mice fed a control diet exhibited a better glucose tolerance than wild-type mice when both were fed the control diet. The better glucose tolerance was accompanied by a significantly lower insulin levels during IPGTT as well as with significantly lower pancreatic islets area and higher muscle and liver Akt phosphorylation 20 min after insulin injection. Altogether, these results suggest that SPAK-KI mice exhibit higher insulin sensibility. Moreover, SPAK-KI mice fed a HFD had lower insulin levels without hyperglycemia or hepatic steatosis than their wild-type littermates, indicating that SPAK inactivation confers a metabolic advantage, even during chronic hypercaloric feeding. It is known that higher insulin levels are associated with an increase in hepatic lipogenesis and adipose tissue accretion (42). An increased hepatic lipogenesis leads to an abnormal lipid deposition in skeletal muscle and to further insulin resistance (45). As a compensatory mechanism, pancreatic β-cells increase in size and insulin release to maintain euglycemia, exacerbating metabolic alterations (46). In this regard, when they were exposed to a HFD, the difference in insulin sensibility became more apparent (Fig. 7*A*). Furthermore, SPAK-KI mice under HFD were protected against islet hypertrophy, as observed in wild-type mice. These observations suggest that the resistance of SPAK-KI mice to diet-induced obesity was also related to a reduction in circulating insulin coupled with enhanced glucose tolerance (Fig. 9).

SPAK is a kinase that has been studied extensively over the last 10 years due to its involvement in blood pressure regula-

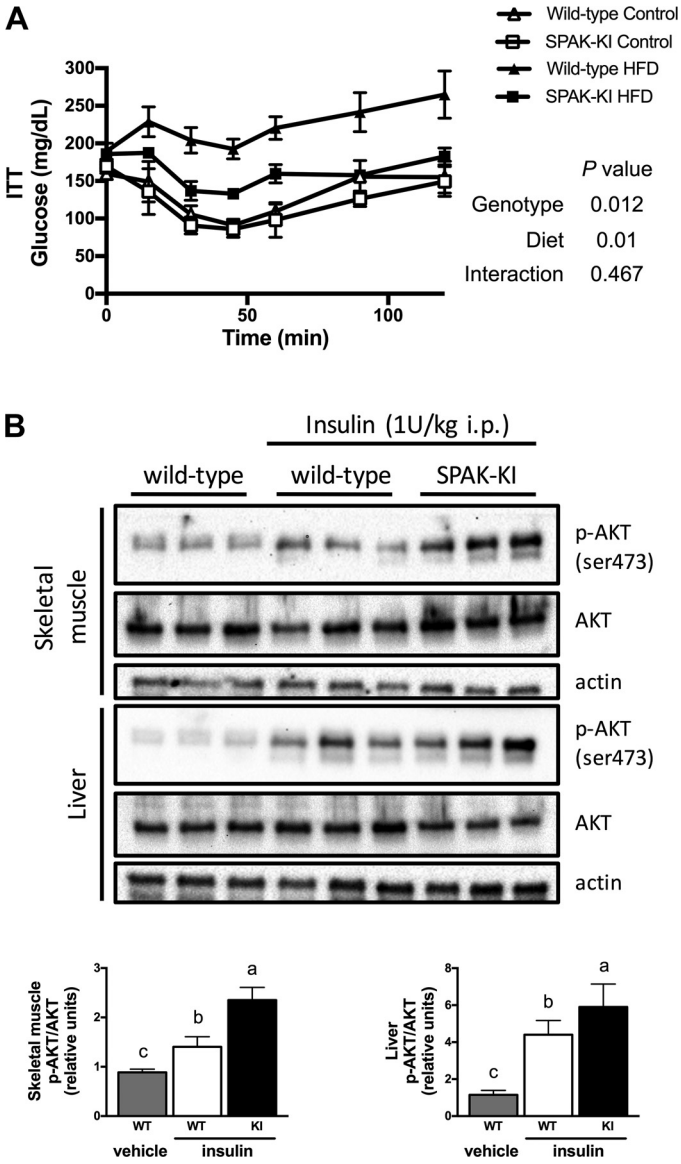


Fig. 8. SPAK-KI mice have an increase in insulin sensitivity. *A*: insulin sensitivity in SPAK-KI mice and their littermate controls was evaluated by an insulin tolerance test (ITT) after 13 wk of being fed a control diet or HFD. *B*: Akt phosphorylation in skeletal muscle and liver of SPAK-KI and wild-type mice 20 min after an ip injection of insulin (1 U/kg body wt) or saline, as evaluated by Akt phosphorylation. Representative blots are shown. The bar graphs represent the mean ± SE of quantitative densitometry from 3 independent experiments. The results are presented as means ± SE. Glucose concentration over time data during the ITT was analyzed using 2-way ANOVA for repeated measures, followed by Bonferroni correction. Immunoblot densitometry quantitation data was analyzed by 1-way parametric analysis of variance (ANOVA), followed by a Bonferroni multiple comparison post hoc test. Different letters denote significant difference between groups ($P < 0.05$), where a > b > c; $n$ = 8–10 mice for each group.

tion (1), as it is the intermediate kinase between the WNKs and the activity of the renal $Na^+$-$Cl^-$ cotransporter (NCC) in the kidneys (47). Our data reveal a previously unrecognized role for SPAK in energy balance regulation and glucose homeostasis. In agreement with this, Takahashi et al. (43) recently observed that WNK4 is increased during adipogenesis and that $WNK4^{-/-}$ mice are also partially resistant to a high-fat-induced obesity.

SPAK phosphorylates and activates the $Na^+$-driven chloride influx (NKCC1 and NKCC2) and inhibits the function of the $K^+$-driven chloride efflux (KCC1–KCC4), members of the SLC12 family of solute carriers in the kidney and the central nervous system. Because the coupled activity of these branches of SLC12 transporters is to modulate the $[Cl^-]_i$, thus, SPAK activity is associated with an increase of $[Cl^-]_i$, whereas SPAK inactivation is associated with decreased $[Cl^-]_i$ (1, 20). The role of $[Cl^-]_i$ in many aspects of intermediate metabolism and thermogenesis has not been explored but is probably involved in several tissues since SPAK is expressed in liver, skeletal muscle, and adipose tissue, in an insulin secreting cell line (Figs. 2*G*, 5*F*, and 7*E*), and in many regions of the central nervous system (1a). There are at least two potential tissues where SPAK modulation of $[Cl^-]_i$ could be of importance for intermediate metabolism and thermogenesis and that could fit with the phenotype observed in this study. One is at the hypothalamus, and the other is the pancreatic β cells.

It is known that the hypothalamus modulates the energy expenditure and thermogenesis in relation to the food intake. Stimulation of the arcuate nucleus (ARH) by several hormones, like leptin, induces signals that synapse in the paraventricular nucleus (PVN) via GABAergic neurons that inhibits the activity of this nucleus upon the solitary tract nucleus (NTS), which then activates the thermogenesis and energy expenditure in the BAT (52). Kong et al. (24) developed mice lacking GABA secretion in RIP-Cre neurons of the ARH, and the resultant phenotype, when fed a HFD, is a mirror image of our SPAK-KI fed a HFD. These mice exhibit an obesity-prone phenotype on a HFD, although their food intake was similar to their wild-type littermates. An increased body weight with augmented fat mass was observed in association with decreased oxygen consumption, UCP1 expression, and BAT activity, with clear BAT transformation into WAT. Given that an absence of GABA secretion from the ARH to the PVN results in an obesity-prone model, due to decreased energy expenditure and thermogenesis (8, 24), it is possible that an exaggerated response to GABA in the PVN results in the opposite phenotype. Given that GABA induces the opening of chloride channels, the effect of this neurotransmitter has an inhibitory effect in adult neurons because the $[Cl^-]_i$ is below its equilibrium potential due to low expression/activity of NKCC1 and high expression/activity of the K-Cl cotransporter KCC2 (5, 13, 30, 41). The lower the $[Cl^-]_i$, the deepest the GABA-induced hyperpolarization. The absence of SPAK activity results in decreased phosphorylation of the SLC12 members (37), a condition that promotes $Cl^-$ efflux and thus a

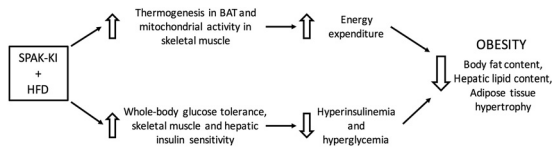


Fig. 9. Metabolic features of SPAK-KI mice associated with protection from HFD-induced obesity. Inactivation of SPAK kinase increases energy expenditure in mice fed a HFD by augmented thermogenesis in brown adipose tissue (BAT) and mitochondrial activity in skeletal muscle. SPAK-KI mice also display increased whole body glucose tolerance associated with increased skeletal muscle and hepatic insulin sensitivity, preventing hyperinsulinemia and hyperglycemia when fed a HFD. All these metabolic features lead to a reduction in hepatic steatosis and fat mass, preventing excessive weight gain even when fed an energy-dense diet.

decrease in $[Cl^-]_i$. It is thus possible that neurons in the PVH of SPAK-KI mice could exhibit upregulation of KCC2 activity, leading to a decrease in $[Cl^-]_i$ and consequently increasing the magnitude of the inhibitory response to GABA. However, further studies will be required to define the $[Cl^-]_i$ and the effect of GABA in PVH neurons of SPAK-KI mice and its consequences in thermogenesis and whole body energy expenditure.

Several studies have suggested that $[Cl^-]_i$ in pancreatic β-cells could be of importance for insulin secretion either because depolarization of the β-cells is required to trigger insulin secretion (2, 3, 7) or because the necessary acidification of the insulin-containing vesicles requires also movement of $Cl^-$ into these vesicles (11, 27). However, the role of $[Cl^-]_i$ in insulin secretion by β-cells has not been completely elucidated. It has been suggested that depolarization of β-cells requires that $[Cl^-]_i$ is above its equilibrium potential (7), suggesting that a high activity of NKCC1 is required. In fact, in the NKCC1-null mouse insulin secretion is sustained due to an unexpected compensatory NKCC2 expression usually not present in β-cells (3), suggesting that the regulation of $[Cl^-]_i$, and thus insulin secretion in β-cells, is a complex process that involves several transporters. This is further supported by the recent observation that β-cells also express the $Cl^-$ extruder KCC2, and pharmacological inhibition of this transporter increases insulin secretion (25). Our SPAK-KI mice would be expected to have a chronic inhibition of NKCC1 and activation of KCC2, potentially decreasing insulin secretion. The observation that high glucose stimulation of INS1E cells increases SPAK phosphorylation supports the proposal that glucose promotes $Cl^-$ efflux from the cells, which in turns triggers SPAK activation. Thus, the role of $[Cl^-]_i$ and SPAK activity for insulin secretion in β-cells is an interesting subject for further investigation. In addition of these two potential mechanisms by which SPAK can modulate energy balance and insulin secretion, our study suggests that SPAK might be involved in the metabolic response for use of different energy substrates in other tissues.

*Conclusions.* Our work indicates that in addition to its well-known role in blood pressure regulation, abrogating SPAK activity generates an elevated energy expenditure and insulin sensitivity phenotype, preventing the increase in adiposity and body weight induced by a high-fat diet. Thus, the pharmacological inhibition of SPAK activity could emerge as a potential strategy to treat obesity and prevent the metabolic derangements associated with weight gain.

## ACKNOWLEDGMENTS

We thank Dr. Dario Alessi of Dundee University(UK) for the donation of the SPAK-KI mouse colony and the anti-SPAK antibodies. We also thank Profs. C. B. Wollheim and Pierre Maechler of the University of Geneva (Switzerland) for kindly providing INS1E cells. We thank Martha Guevara-Cruz for assistance with statistical analysis.

## GRANTS

This work was supported by grant no. 23 of the "Fronteras de la Ciencia" program of the National Council of Science and Technology Mexico to G. Gamba. G. Gamba is the guarantor of this study.

## DISCLOSURES

No conflicts of interest, financial or otherwise, are declared by the authors.

## AUTHOR CONTRIBUTIONS

I.T.-V., L.G.C.-P., L.G.N., N.T., N.A.B., A.R.T., and G.G. conceived and designed research; I.T.-V., L.G.C.-P., L.G.N., J.V.J., N.U., M.C.-C., C.T.-P., and B.A.M.-G. performed experiments; I.T.-V., L.G.C.-P., L.G.N., J.V.J., N.U., M.C.-C., B.A.M.-G., and G.G. analyzed data; I.T.-V., L.G.C.-P., L.G.N., J.V.J., N.U., M.C.-C., C.T.-P., B.A.M.-G., N.T., N.A.B., A.R.T., and G.G. interpreted results of experiments; I.T.-V., L.G.C.-P., C.T.-P., B.A.M.-G., and G.G. prepared figures; I.T.-V., L.G.C.-P., and G.G. drafted manuscript; I.T.-V., L.G.C.-P., L.G.N., J.V.J., N.U., M.C.-C., N.T., N.A.B., A.R.T., and G.G. edited and revised manuscript; I.T.-V., L.G.C.-P., L.G.N., J.V.J., N.U., M.C.-C., C.T.-P., B.A.M.-G., N.T., N.A.B., A.R.T., and G.G. approved final version of manuscript.

## REFERENCES

1. **Alessi DR, Zhang J, Khanna A, Hochdörfer T, Shang Y, Kahle KT.** The WNK-SPAK/OSR1 pathway: master regulator of cation-chloride cotransporters. *Sci Signal* 7: re3, 2014. doi:10.1126/scisignal.2005365.

1a. **Allen Institute.** *Allen Brain Atlas* (Online). http://mouse.brain-map.org/gene/show/32896 [2017].

2. **Alshahrani S, Almutairi MM, Kursan S, Dias-Junior E, Almiahuob MM, Aguilar-Bryan L, Di Fulvio M.** Increased Slc12a1 expression in β-cells and improved glucose disposal in Slc12a2 heterozygous mice. *J Endocrinol* 227: 153–165, 2015. doi:10.1530/JOE-15-0327.

3. **Alshahrani S, Di Fulvio M.** Enhanced insulin secretion and improved glucose tolerance in mice with homozygous inactivation of the Na(+)K(+)2Cl(−) co-transporter 1. *J Endocrinol* 215: 59–70, 2012. doi:10.1530/JOE-12-0244.

4. **Arqués O, Chicote I, Tenbaum SP, Puig I, Palmer H.** Standardized Relative Quantification of Immunofluorescence Tissue Staining. *Protoc Exchange* 1–5, 2012.

5. **Arroyo JP, Kahle KT, Gamba G.** The SLC12 family of electroneutral cation-coupled chloride cotransporters. *Mol Aspects Med* 34: 288–298, 2013. doi:10.1016/j.mam.2012.05.002.

6. **Alli Shaik A, Qiu B, Wee S, Choi H, Gunaratne J, Tergaonkar V.** Phosphoprotein network analysis of white adipose tissues unveils deregulated pathways in response to high-fat diet. *Sci Rep* 6: 25844, 2016.[Erratum in Sci Rep 6: 27230, 2016.] doi:10.1038/srep25844.

7. **Best L.** Glucose-induced electrical activity in rat pancreatic beta-cells: dependence on intracellular chloride concentration. *J Physiol* 568: 137–144, 2005. doi:10.1113/jphysiol.2005.093740.

8. **Bouret SG.** RIPping off GABA release in hypothalamic circuits causes obesity. *Cell Metab* 16: 557–558, 2012. doi:10.1016/j.cmet.2012.10.014.

9. **Cervantes-Perez LG, Castaneda-Bueno M, Jimenez JV, Vazquez N, Rojas-Vega L, Alessi DR, Bobadilla NA, Gamba G.** Disruption of the with no lysine kinase-STE20-proline alanine-rich kinase pathway reduces the hypertension induced by angiotensin II. 2017 September 9 [Epub ahead of print]. doi:10.1097/HJH.0000000000001554.

10. **Chouchani ET, Kazak L, Jedrychowski MP, Lu GZ, Erickson BK, Szpyt J, Pierce KA, Laznik-Bogoslavski D, Vetrivelan R, Clish CB, Robinson AJ, Gygi SP, Spiegelman BM.** Mitochondrial ROS regulate thermogenic energy expenditure and sulfenylation of UCP1. *Nature* 532: 112–116, 2016. doi:10.1038/nature17399.

11. **Deriy LV, Gomez EA, Jacobson DA, Wang X, Hopson JA, Liu XY, Zhang G, Bindokas VP, Philipson LH, Nelson DJ.** The granular chloride channel ClC-3 is permissive for insulin secretion. *Cell Metab* 10: 316–323, 2009. doi:10.1016/j.cmet.2009.08.012.

12. **Engfeldt P, Arner P.** Lipolysis in human adipocytes, effects of cell size, age and of regional differences. *Horm Metab Res Suppl* 19: 26–29, 1988.

13. **Friedel P, Kahle KT, Zhang J, Hertz N, Pisella LI, Buhler E, Schaller F, Duan J, Khanna AR, Bishop PN, Shokat KM, Medina I.** WNK1-regulated inhibitory phosphorylation of the KCC2 cotransporter maintains the depolarizing action of GABA in immature neurons. *Sci Signal* 8: ra65, 2015. doi:10.1126/scisignal.aaa0354.

14. **Friedman JM, Halaas JL.** Leptin and the regulation of body weight in mammals. *Nature* 395: 763–770, 1998. doi:10.1038/27376.

15. **Gagnon KB, Delpire E.** Molecular physiology of SPAK and OSR1: two Ste20-related protein kinases regulating ion transport. *Physiol Rev* 92: 1577–1617, 2012. doi:10.1152/physrev.00009.2012.

16. **Galarraga M, Campión J, Muñoz-Barrutia A, Boqué N, Moreno H, Martínez JA, Milagro F, Ortiz-de-Solórzano C.** Adiposoft: automated software for the analysis of white adipose tissue cellularity in histological sections. *J Lipid Res* 53: 2791–2796, 2012. doi:10.1194/jlr.D023788.

17. **Gamba G.** Molecular physiology and pathophysiology of electroneutral cation-chloride cotransporters. *Physiol Rev* 85: 423–493, 2005. doi:10.1152/physrev.00011.2004.
18. **Gao M, Ma Y, Liu D.** High-fat diet-induced adiposity, adipose inflammation, hepatic steatosis and hyperinsulinemia in outbred CD-1 mice. *PLoS One* 10: e0119784, 2015. doi:10.1371/journal.pone.0119784.
19. **Glastras SJ, Chen H, Teh R, McGrath RT, Chen J, Pollock CA, Wong MG, Saad S.** Mouse Models of Diabetes, Obesity and Related Kidney Disease. *PLoS One* 11: e0162131, 2016. doi:10.1371/journal.pone.0162131.
20. **Hadchouel J, Ellison DH, Gamba G.** Regulation of Renal Electrolyte Transport by WNK and SPAK-OSR1 Kinases. *Annu Rev Physiol* 78: 367–389, 2016. doi:10.1146/annurev-physiol-021115-105431.
21. **Hsu SM, Raine L, Fanger H.** Use of avidin-biotin-peroxidase complex (ABC) in immunoperoxidase techniques: a comparison between ABC and unlabeled antibody (PAP) procedures. *J Histochem Cytochem* 29: 577–580, 1981. doi:10.1177/29.4.6166661.
22. **Huang T, Hu FB.** Gene-environment interactions and obesity: recent developments and future directions. *BMC Med Genomics* 8, *Suppl* 1: S2, 2015. doi:10.1186/1755-8794-8-S1-S2.
23. **Kim J, Lee T, Kim TH, Lee KT, Kim H.** An integrated approach of comparative genomics and heritability analysis of pig and human on obesity trait: evidence for candidate genes on human chromosome 2. *BMC Genomics* 13: 711, 2012. doi:10.1186/1471-2164-13-711.
24. **Kong D, Tong Q, Ye C, Koda S, Fuller PM, Krashes MJ, Vong L, Ray RS, Olson DP, Lowell BB.** GABAergic RIP-Cre neurons in the arcuate nucleus selectively regulate energy expenditure. *Cell* 151: 645–657, 2012. doi:10.1016/j.cell.2012.09.020.
25. **Kursan S, McMillen TS, Beesetty P, Dias-Junior E, Almutairi MM, Sajib AA, Kozak JA, Aguilar-Bryan L, Di Fulvio M.** The neuronal K+Cl- co-transporter 2 (Slc12a5) modulates insulin secretion. *Sci Rep* 7: 1732, 2017. doi:10.1038/s41598-017-01814-0.
26. **Leal-Díaz AM, Noriega LG, Torre-Villalvazo I, Torres N, Alemán-Escondrillas G, López-Romero P, Sánchez-Tapia M, Aguilar-López M, Furuzawa-Carballeda J, Velázquez-Villegas LA, Avila-Nava A, Ordáz G, Gutiérrez-Uribe JA, Serna-Saldivar SO, Tovar AR.** Aguamiel concentrate from Agave salmiana and its extracted saponins attenuated obesity and hepatic steatosis and increased Akkermansia muciniphila in C57BL6 mice. *Sci Rep* 6: 34242, 2016. doi:10.1038/srep34242.
27. **Li DQ, Jing X, Salehi A, Collins SC, Hoppa MB, Rosengren AH, Zhang E, Lundquist I, Olofsson CS, Mörgelin M, Eliasson L, Rorsman P, Renström E.** Suppression of sulfonylurea- and glucose-induced insulin secretion in vitro and in vivo in mice lacking the chloride transport protein ClC-3. *Cell Metab* 10: 309–315, 2009. doi:10.1016/j.cmet.2009.08.011.
28. **Lusk G.** *The Elements of the Science of Nutrition*. Philadelphia, PA: Saunders, 1906.
29. **Mather K.** Surrogate measures of insulin resistance: of rats, mice, and men. *Am J Physiol Endocrinol Metab* 296: E398–E399, 2009. doi:10.1152/ajpendo.90889.2008.
30. **Medina I, Friedel P, Rivera C, Kahle KT, Kourdougli N, Uvarov P, Pellegrino C.** Current view on the functional regulation of the neuronal K(+)-Cl(−) cotransporter KCC2. *Front Cell Neurosci* 8: 27, 2014. doi:10.3389/fncel.2014.00027.
31. **Mehlem A, Hagberg CE, Muhl L, Eriksson U, Falkevall A.** Imaging of neutral lipids by oil red O for analyzing the metabolic status in health and disease. *Nat Protoc* 8: 1149–1154, 2013. doi:10.1038/nprot.2013.055.
32. **Merglen A, Theander S, Rubi B, Chaffard G, Wollheim CB, Maechler P.** Glucose sensitivity and metabolism-secretion coupling studied during two-year continuous culture in INS-1E insulinoma cells. *Endocrinology* 145: 667–678, 2004. doi:10.1210/en.2003-1099.
33. **Montgomery MK, Turner N.** Mitochondrial dysfunction and insulin resistance: an update. *Endocr Connect* 4: R1–R15, 2015. doi:10.1530/EC-14-0092.
34. **Nielsen TS, Jessen N, Jørgensen JO, Møller N, Lund S.** Dissecting adipose tissue lipolysis: molecular regulation and implications for metabolic disease. *J Mol Endocrinol* 52: R199–R222, 2014. doi:10.1530/JME-13-0277.
35. **Noriega-López L, Tovar AR, Gonzalez-Granillo M, Hernández-Pando R, Escalante B, Santillán-Doherty P, Torres N.** Pancreatic insulin secretion in rats fed a soy protein high fat diet depends on the interaction between the amino acid pattern and isoflavones. *J Biol Chem* 282: 20657–20666, 2007. doi:10.1074/jbc.M701045200.
36. **Pinkert CA.** *Transgenic Animal Technology: A Laboratory Handbook*. London, UK: Elsevier Science, 2014.
37. **Rafiqi FH, Zuber AM, Glover M, Richardson C, Fleming S, Jovanović S, Jovanović A, O'Shaughnessy KM, Alessi DR.** Role of the WNK-activated SPAK kinase in regulating blood pressure. *EMBO Mol Med* 2: 63–75, 2010. doi:10.1002/emmm.200900058.
38. **Rodríguez-Rodríguez C, Torres N, Gutiérrez-Uribe JA, Noriega LG, Torre-Villalvazo I, Leal-Díaz AM, Antunes-Ricardo M, Márquez-Mota C, Ordaz G, Chavez-Santoscoy RA, Serna-Saldivar SO, Tovar AR.** The effect of isorhamnetin glycosides extracted from Opuntia ficus-indica in a mouse model of diet induced obesity. *Food Funct* 6: 805–815, 2015. doi:10.1039/C4FO01092B.
39. **Scherer PE, Hill JA.** Obesity, Diabetes, and Cardiovascular Diseases: a compendium. *Circ Res* 118: 1703–1705, 2016. doi:10.1161/CIRCRESAHA.116.308999.
41. **Shekarabi M, Zhang J, Khanna AR, Ellison DH, Delpire E, Kahle KT.** WNK Kinase Signaling in Ion Homeostasis and Human Disease. *Cell Metab* 25: 285–299, 2017. doi:10.1016/j.cmet.2017.01.007.
42. **Steneberg P, Sykaras AG, Backlund F, Straseviciene J, Söderström I, Edlund H.** Hyperinsulinemia enhances hepatic expression of the fatty acid transporter Cd36 and provokes hepatosteatosis and hepatic insulin resistance. *J Biol Chem* 290: 19034–19043, 2015. doi:10.1074/jbc.M115.640292.
43. **Takahashi D, Mori T, Sohara E, Tanaka M, Chiga M, Inoue Y, Nomura N, Zeniya M, Ochi H, Takeda S, Suganami T, Rai T, Uchida S.** WNK4 is an adipogenic factor and its deletion reduces diet-induced obesity in mice. *EBioMedicine* 18: 118–127, 2017. doi:10.1016/j.ebiom.2017.03.011.
44. **Trujillo J, Ramírez V, Pérez J, Torre-Villalvazo I, Torres N, Tovar AR, Muñoz RM, Uribe N, Gamba G, Bobadilla NA.** Renal protection by a soy diet in obese Zucker rats is associated with restoration of nitric oxide generation. *Am J Physiol Renal Physiol* 288: F108–F116, 2005. doi:10.1152/ajprenal.00077.2004.
45. **Unger RH, Clark GO, Scherer PE, Orci L.** Lipid homeostasis, lipotoxicity and the metabolic syndrome. *Biochim Biophys Acta* 1801: 209–214, 2010. doi:10.1016/j.bbalip.2009.10.006.
46. **Unger RH, Scherer PE.** Gluttony, sloth and the metabolic syndrome: a roadmap to lipotoxicity. *Trends Endocrinol Metab* 21: 345–352, 2010. doi:10.1016/j.tem.2010.01.009.
47. **Vitari AC, Deak M, Morrice NA, Alessi DR.** The WNK1 and WNK4 protein kinases that are mutated in Gordon's hypertension syndrome phosphorylate and activate SPAK and OSR1 protein kinases. *Biochem J* 391: 17–24, 2005. doi:10.1042/BJ20051180.
48. **Vlasova M, Purhonen AK, Jarvelin MR, Rodilla E, Pascual J, Herzig KH.** Role of adipokines in obesity-associated hypertension. *Acta Physiol (Oxf)* 200: 107–127, 2010. doi:10.1111/j.1748-1716.2010.02171.x.
49. **Wang J, Zhu Y, Jing J, Chen Y, Mai J, Wong SH, O'Reilly J, Ma L.** Relationship of BMI to the incidence of hypertension: a 4 years' cohort study among children in Guangzhou, 2007-2011. *BMC Public Health* 15: 782, 2015. doi:10.1186/s12889-015-1997-6.
50. **Wang Y, O'Connell JR, McArdle PF, Wade JB, Dorff SE, Shah SJ, Shi X, Pan L, Rampersaud E, Shen H, Kim JD, Subramanya AR, Steinle NI, Parsa A, Ober CC, Welling PA, Chakravarti A, Weder AB, Cooper RS, Mitchell BD, Shuldiner AR, Chang YP.** From the Cover: Whole-genome association study identifies STK39 as a hypertension susceptibility gene. *Proc Natl Acad Sci USA* 106: 226–231, 2009. doi:10.1073/pnas.0808358106.
51. **Wasada T, Kasahara T, Wada J, Jimba S, Fujimaki R, Nakagami T, Iwamoto Y.** Hepatic steatosis rather than visceral adiposity is more closely associated with insulin resistance in the early stage of obesity. *Metabolism* 57: 980–985, 2008. doi:10.1016/j.metabol.2008.02.015.
52. **Zhang W, Bi S.** Hypothalamic regulation of brown adipose tissue thermogenesis and energy homeostasis. *Front Endocrinol (Lausanne)* 6: 136, 2015. doi:10.3389/fendo.2015.00136.